Optimization of the P′-Region of Peptide Inhibitors of Hepatitis C Virus NS3/4A Protease

Paolo Ingallinella, Elisabetta Bianchi, Raffaele Ingenito, Uwe Koch, Christian Steinkühler, Sergio Altamura, and Antonello Pessi*

IRBM P. Angeletti, Via Pontina km 30.600, 00040 Pomeza, Rome, Italy

Received July 10, 2000

ABSTRACT: Infection by Hepatitis C Virus (HCV) leads to a slowly progressing disease that over two decades can lead to liver cirrhosis or liver cancer. Currently, one of the most promising approaches to anti-HCV therapy is the development of inhibitors of the NS3/4A protease, which is essential for maturation of the viral polyprotein. Several substrate-derived inhibitors of NS3/4A have been described, all taking advantage of binding to the S subsite of the enzyme. Inspection of the S′ subsite of NS3/4A shows binding pockets which might be exploited for inhibitor binding, but due to the fact that ground-state binding to the S′ subsite is not used by the substrate, this does not represent a suitable starting point. We have now optimized S′-binding in the context of noncleavable decapeptides spanning P6−P4′. Binding was sequentially increased by introduction of the previously optimized P-region [Ingallinella et al. (1998) *Biochemistry 37,* 8906−8914], change of the P4′ residue, and combinatorial optimization of positions P2′−P3′. The overall process led to an increase in binding of more than 3 orders of magnitude, with the best decapeptide showing IC_{50} < 200 pM. The binding mode of the decapeptides described in the present work shares features with the binding mode of the natural substrates, together with novel interactions within the S′ subsite. Therefore, these peptides may represent an entry point for a novel class of NS3 inhibitors.

Hepatitis C is a slowly progressing viral infection that over two decades can lead to liver cirrhosis or liver cancer. Infection by Hepatitis C virus (HCV)[1] is widely recognized today as a huge public health concern, with more than 170 million people infected worldwide, most of them unknowingly, while neither a generally effective treatment nor a preventive vaccine is available (*1*, *2*). Currently, one of the most promising approaches to anti-Hepatitis C Virus therapy is the development of inhibitors of the virally encoded protease NS3, which is essential for the maturation of the HCV polyprotein. The chymotrypsin-like serine proteinase domain is contained within the N-terminal 180 amino acids of NS3, residues 1027−1206 of the polyprotein (*3*−*8*). The C-terminal portion of the protein contains an RNA helicase and an RNA-stimulated NTPase (*9*). Although the NS3 proteinase has proteolytic activity of its own, interaction with a second viral protein, NS4A, is essential for efficient processing of all the NS3-dependent polyprotein cleavage sites (*3*, *4*, *10*). Accordingly, it is now more common to refer to this proteinase as the NS3/4A protease.

Recently, we (*11*, *12*) as well as others (*13*, *14*) reported on the discovery of potent peptide inhibitors derived from the N-terminal region of the substrate upon cleavage by NS3/4A ("product inhibitors"). Apart for the binding energy extracted from the C-terminal carboxylate, the interaction of these inhibitors with NS3/4A is similar to the substrate, including binding in the S1 pocket and the prominent electrostatic interaction of the P6−P5[2] acidic couple. This finding is consistent with the previous observation that the main determinants of ground-state substrate binding to the enzyme (reflected in the K_m) reside in the P-region (*11*, *15*−*17*).

At variance with the P region, the P′ region of the substrate, while being important for catalysis, contributes little to ground-state binding to the enzyme (*15*−*17*). Accordingly, peptides based on the P′ regions of the natural substrates (spanning residues P1′ up to P10′) do not inhibit NS3/4A to any significant extent (*12*, *18*). This notwithstanding, inspection of the crystal structure of the NS3 protease domain with or without 4A (*19*−*21*), of the NMR structure of the protease domain (*22*) and more recently of

* To whom correspondence should be addressed. Phone: +39-6-91093445. Fax: +39-6-91093482. E-mail: pessi@irbm.it.

[1] Abbreviations: CHAPS, 3-(3-cholamidopropyl)dimethylammonio-1-propanesulfonate; DIEA, diisopropylethylamine; DMAP, *N*′*N*′-(dimethylamino)-pyridine; DMF, *N*,*N*′-dimethylformamide; DMSO, dimethyl sulfoxide; DTT, dithiothreitol; Fmoc, 9-fluorenylmethyloxycarbonyl; HCV, (human) hepatitis C virus; HATU, *O*-(7-azabenzotriazol-1-yl)-1,1,3,3-tetramethyluronium hexafluorophosphate; HOBt, *N*-hydroxybenzotriazole; Pep4AK, amino acids 1678−1691 of the HCV polyprotein sequence encompassing the central hydrophobic domain of the NS4A protein sufficient for NS3 activation, with three additional non-HCV N-terminal lysine residues, sequence KKKGSVVIVGRI-ILSGR-NH_2; PyBOP, benzotriazole-1-yl-oxy-tris-pyrrolidino-phosphonium hexafluorophosphate; t-Bu, *tert*-butyl; TFA, trifluoroacetic acid; TNBS, trinitrobenzenesulfonic acid.

[2] We follow the nomenclature of Schechter and Berger [Schechter, I., and Berger, A. (1967) *Biochem. Biophys. Res. Commun. 27,* 157−162] in designating the cleavage sites as P6−P5−P4−P3−P2−P1...P1′−P2′−P3′−P4′, etc., with the scissile bond between P1 and P1′ and the C-terminus of the substrate on the prime site. The binding sites on the enzyme corresponding to residues P6−P5−P4−P3−P2−P1...P1′−P2′−P3′−P4′ are indicated as S6−S5−S4−S3−S2−S1...S1′−S2′−S3′−S4′, etc.

10.1021/bi001590g CCC: $19.00 © 2000 American Chemical Society
Published on Web 09/27/2000

the crystal structure of the whole NS3/4A protein (*23*) shows the presence of binding pockets in the S′ region which might be exploited for binding of active-site directed inhibitors. A ligand taking advantage of S′-binding could therefore display a range of interactions with the enzyme different from the ones used by the substrate, and represent a novel class of NS3/4A inhibitors.

In the present work, we have optimized S′-binding in the context of noncleavable decapeptides spanning P6−P4′. Using single analogues and combinatorial libraries, we have produced decapeptides with IC_{50} < 200 pM.

MATERIALS AND METHODS

Peptides Synthesis. Protected amino acids were commercially available from Novabiochem (Läufelfingen), Bachem (Bubendorf), Neosystem (Strasbourg), or Synthetech (Albany). Peptide synthesis was performed by Fmoc/t-Bu chemistry (*24*) on Novasyn TGA (peptide acids) or Novasyn TGR (peptide amides) resin. The first residue of the C-terminal acids was esterified to the resin in the presence of DMAP (*24*). Individual peptide sequences were assembled on a Millipore 9050 Plus synthesizer, using PyBOP/HOBt/DIEA (1:1:2) activation, 5-fold excess of acylants over the resin amino groups and a coupling time of 30−60 min. Multiple peptide synthesis and the assembly of combinatorial libraries were performed on a Zinsser SMPS 350 synthesizer using PyBOP/HOBt/DIEA (1:1:2) activation, 5-fold excess of acylants, and a coupling time of 20−120 min as judged by the standard ninhydrin and TNBS color tests, essentially as described (*25*−*28*). The undefined or "mixed" positions were incorporated by coupling a mixture of activated amino acids, with the relative ratios suitably adjusted to compensate for the differences in reactivity (*27*); near equivalence of the incorporation was assessed by quantitative amino acid analysis. The peptides were cleaved with TFA 88%, phenol 5%, triisopropylsilane 2%, water 5% (reagent B, ref *29*). Crude peptides were purified by reversed-phase HPLC on a Nucleosyl C-18, 250 × 21 mm, 100 Å, 7 μm, using H_2O, 0.1% TFA, and acetonitrile, 0.1% TFA, as eluents. Analytical HPLC was performed on a Ultrasphere C-18, 250 × 4.6 mm, 80 Å, 5 μm (Beckman). Purified (>95%) peptides were characterized by mass spectrometry, [^{1}H]-NMR and amino acid analysis.

Enzyme Preparations and Site-Directed Mutagenesis. The protease domain of the HCV J strain NS3 protein (amino acids 1027−1206, followed by the sequence ASKKKK) was prepared and purified as previously described (*12*). Single-mutant enzymes, carrying either the Lys136Met or the Arg109Gln amino acid change, were produced to analyze the importance of these two residues for inhibitor binding, in particular, in position P3′ (see later). The two mutations were introduced by PCR using appropriate mutagenic primers. Clones were fully sequenced on both strands to exclude the introduction of additional mutations by PCR. All enzymes were purified and quality-controlled as previously described (*12*, *30*). Enzyme stocks were quantitated by amino acid analysis, shock-frozen in liquid nitrogen and kept in aliquots at −80 °C until use.

Protease Activity Assays. Concentration of stock solutions of peptides, prepared in DMSO or in buffered aqueous solutions and kept at −80 °C until use, was determined by quantitative amino acid analysis performed on HCl-hydrolyzed samples. The HPLC enzymatic assay was performed as described in refs *11* and *12*. The protease cofactor was a peptide spanning the central hydrophobic core of the NS4A protein, with a three-lysine tag at the N-terminus to increase solubility (*31*) Pep4AK (KKKGSVVIVGRIILSGR-NH_2). Potencies in the low nanomolar to subnanomolar range were determined with the fluorescent substrate Ac-DEMEE-**CA**SHLPYE(EDANS)-NH_2 that allows the use of 150 pM enzyme in the assay. For the experiments at high ionic strength enzyme, activity was determined using the substrate EAGDDIVP**CS**MSYTWGA-OH, based on the sequence of the NS5A/5B cleavage site of the HCV polyprotein. Assays were done using 0.2−1 nM NS3 protease in 50 mM Hepes, pH 7.5, 1 mM DTT, 15% glycerol, 150 mM NaCl, 1% CHAPS, containing 80 mM Pep4AK and analyzed as previously described (*11*, *12*). The microplate assay is described in detail in ref *32*.

Modeling of the Substrate NS3/4A−Protease Complex. Models of the complex between the decapeptide Ac-Asp-Glu-Dif-Ile-Cha-Cys-Pro-Cha-Asp-Leu-NH_2 (Dif, 3,3-diphenylalanine; Cha, β-cyclohexyl-alanine) and NS3/Pep4A were constructed using energy minimization and molecular dynamics. All calculations were carried out with the program BatchMin and the molecular modeling package Insight II/Discover (Biosym Technologies Inc., San Diego, CA). Hydrogen atoms were included, and the potential energy of the complex was expressed by the force field MMFF (*33*) as implemented in the MacroModel V5.0 distribution of the simulation program Batchmin. No nonbonded or Coulombic cutoffs were used and the dielectric constant was set to 1.0. NMR data for the hexapeptide product inhibitor (*34*) were used to define the interactions and conformation of the P-site portion of the substrate. The P-site of the decapeptide was docked onto NS3, and the P′-site of the substrate was attached in an extended conformation. The P′-site conformation was optimized by a combination of molecular dynamics and energy minimization of the substrate docked into the substrate binding region.

At variance with the S-subsite, the organization of the S′-region as defined by modeling strongly depends on the presence of NS4A. Comparison of the crystal structures of NS3/4A in the absence and presence of ketoacids which bind to the S-subsite shows no significant influence on the S′-region (*35*). Larger changes, however, are to be expected upon binding of the decapeptide inhibitors. In the absence of structural data on the complex, our modeling gains significance from the good correlation between the structure−activity relationship [SAR] predicted from the model and the one observed experimentally (see later).

RESULTS

Development of Peptide Inhibitors Spanning P6−P4′. Since we found no activity in any of the peptides corresponding to the isolated P′-region (*12*), optimization of the S′-binding region was pursued in the context of noncleavable decapeptides spanning P6−P4′. To stabilize the scissile bond toward hydrolysis, we studied two types of modifications in P1′: *N*-methylation of the natural residue (Ala from the NS4A/4B cleavage site) and substitution with a secondary amino acid (1,2,3,4-tetrahydroisoquinoline-3-carboxylic acid

Table 1: IC_{50} Values for Cleavable and Noncleavable[a] Decapeptide Inhibitors

	peptide[b,c]	IC_{50} (μM)
	cleaved by NS3/4A	
1.	Ac-GluAspValValAbuCys(Me)AlaNleSerTyr-NH_2	3.5
2.	Ac−AspGluDifIleChaCys(Me)AlaSerHisLeu-NH_2	3.4
3.	Ac-GluAspValValAbuCysTicNleSerTyr-NH_2	1.9
4.	Ac-GluAspValValLeuCysTicNleSerTyr-NH_2	1
5.	Ac−Asp-D-GluLeuIleChaCys(Me)AlaSerHisLeu-NH_2	0.6
6.	Ac−AspGluDifIleChaCys(Me)AlaNleSerTyr-NH_2	0.2
7.	Ac−AspGluDifIleChaCysTicNleSerTyr-NH_2	0.1
	not-cleaved by NS3/4A[a]	
8.	Ac-GluAspValValAbuCysProNleSerTyr-NH_2	8.5
9.	Ac−AspGluDifIleChaAbu(Me)AlaSerHisLeu-NH_2	29
10.	Ac−AspGluDifIleCha(Me)AbuAlaSerHisLeu-NH_2	8
11.	Ac-AspGluDifIleCha(Me)Abu(Me)AlaSerHisLeu-NH_2	3.8
12.	Ac-Asp-D-GluLeuIleChaAbu(Me)AlaSerHisLeu-NH_2	5
13.	Ac-Asp-D-GluLeuIleCha(Me)Abu(Me)AlaSerHisLeu-NH_2	3.1
14.	Ac-AspGluDifIleChaCysProNleSerTyr-NH_2	0.9
15.	Ac-AspGluDifIleChaCysProNleSerLeu-NH_2	0.1

[a] $K_{cat}/K_m < 100\ M^{-1}\ s^{-1}$. [b] Abbreviations: Abu, α-aminobutyric acid; Nle, Norleucine; Dif, 3,3-diphenylalanine; Cha, β-cyclohexylalanine; Tic, 1,2,3,4-tetrahydroisoquinoline-3-L-carboxylic acid. [c] N-Methylation of the amide nitrogen is indicated as (Me) preceding the three-letter code of the amino acid.

= Tic, and proline), as reported by Landro et al. (*16*). As shown in Table 1, peptides with P1 = Cys and P1′ = *N*-methyl-alanine are still cleaved, albeit very slowly, by NS3/4A (peptides 1, 2, 5, and 6). *N*-Methylation prevents hydrolysis in the context of a suboptimal P1 (Abu, peptides 9 and 12). *N*-Methylation in P1 (with or without concomitant *N*-methylation in P1′) is also effective (peptides 10, 11, and 13). For secondary amino acids, although we confirmed the finding of Landro et al. that P1′ = Tic gives a more potent inhibitor with respect to P1′ = Pro (compare peptides 3 and 8, 7 and 14), we also found that peptides with P1′ = Tic (but not those with P1′ = Pro) are slowly hydrolyzed by the enzyme. The observed 10-fold difference in potency between peptide 7 and 14 might therefore be due at least in part to the generation in situ of a potent product inhibitor (IC_{50} for Ac-Asp-Glu-Dif-Ile-Cha-Cys-OH is 0.06 μM, ref *12*, Dif = 3,3-diphenyl-alanine, Cha = β-cyclohexyl-alanine). From the above considerations, and also taking into account the ease of synthesis of the corresponding decapeptides (to ensure a more consistent quality of all the library members), for subsequent work we selected P1′ = Pro.

Development of the Parent Noncleavable Decapeptide for Combinatorial Optimization. Our previous experience with combinatorial libraries (*11*, *27*, *28* and unpublished data) had shown that we could unambiguously assess the relative potency of the library pools in a straightforward manner only when the parent compound showed potency at least in the low micromolar range. Therefore, we (arbitrarily) set our threshold potency for a suitable parent decapeptide as IC_{50} < 500 nM. Starting from the decapeptide of Landro et al. (*16*) (peptide 8, Table 1), we first introduced the P-region residues, which had been optimized for the product inhibitors (*11*); the resulting peptide (peptide 14, Table 1) showed a 10-fold improvement in potency. We then changed the P4′ residue from Tyr (NS5A/NS5B cleavage site) to Leu (NS4A/NS4B cleavage site). The rationale for this was the established importance of P4′ for catalysis (*15*−*17*), most likely as a contact for the NS4A cofactor (*16*) and our previous experiment of reverse alanine scanning on the NS4A/4B substrate (*15*). We had studied the effect of reintroducing P4′-Leu in a minimalist analogue (DEAEACAAA**A**PYK) of the NS4A/4B cleavage site (DEMEECASHLPYK). The resulting peptide (DEAEACAAA**L**PYK) showed a 10-fold increase in turnover, resulting from a 3.3-fold increase in k_{cat} and a 3.1-fold decrease in K_m. Moreover, we had observed that in this series P4′-Leu gave 4-fold more turnover than P4′-Tyr. The peptide inhibitor resulting from the Tyr-to-Leu substitution in P4′ (peptide 15, Table 1) showed a further 10-fold increase in potency, and with IC_{50} = 60 nM, it was now a good starting point for combinatorial optimization.

Combinatorial Optimization of Positions P2′−*P3′.* On the basis of Ac-Asp-Glu-Dif-Ile-Cha-Cys-Pro-Nle-Ser-Leu-NH_2, (Nle = norleucine), we prepared a $P_2'-P_3'$ combinatorial library in the format Ac-Asp-Glu-Dif-Ile-Cha-Cys-Pro-**Ooo-Xxx**-Leu-NH_2 with Ooo and Xxx defined as in Houghten et al. (*36*): Ooo = defined amino acid, one of a panel of 91 amino acids, and Xxx = mixed position, anyone of the amino acids of the same panel (Table 2). Overall, the library was composed of 91 mixtures of 91 peptides each. The peptides were tested as crude products coming from cleavage, in the microplate assay at a final concentration of 1 μM. As shown in Figure 1, position P2′ is best occupied by hydrophobic amino acids, either aliphatic or aromatic, including the parent residue Nle; polar, charged, and conformationally constrained amino acids are strongly disfavored, and the D-chirality is absolutely not allowed. The best pools were (in this order) β-cyclohexylalanine (Cha), phenylglycine (Phg), homophenylalanine (Hof) and norleucine (Nle). Titration curves for these pools yielded IC_{50}s of 85 nM, 88 nM, 120nM and 156 nM, respectively.

Since these values were very close to each other, instead of choosing a single amino acid, we used a mixture of these four residues in the P2′ position. The resulting library was Ac-AspGluDifIleChaCysPro[**Cha/Phg/Hof/Nle]Ooo**Leu-NH_2, composed of 91 mixtures of four peptides each, which were tested at a lower concentration (200 nM) than the previous library (Figure 2). Polar residues are preferred in this position, like Asn, Gln, Thr, Hyp (hydroxyproline), and methionine sulfoxide, and including the parent residue Ser. The best result, however, was obtained with the acidic amino acids. Titration curves for the best pools gave IC_{50} values of 16, 17, 20, 24, 31, and 33 nM for Asp, Glu, Gla (γ-carboxyglutamic acid), Gln, Asn, and Hyp, respectively.

Single peptides were then prepared which corresponded to the combination of the best residues in P2′ and P3′. From the data in Table 3, it is apparent that the contributions of the residues in these two positions are additive and not synergic: the rank order for the best residue in P3′ is the same, Asp > Hyp > Gln > Ser, with either P2′ = Nle (peptide 4, 3, 2, and 1), Cha (peptides 9, 8, or 7), or Hof (peptides 12, 11, or 10). Likewise, the rank order for the P2′ residues Cha and Nle (Cha > Nle) is maintained between P3′ = Asp (peptides 9 and 4) and P3′ = Ser (peptides 5 and 1).

SAR of the P−*P′ Inhibitors.* The most active decapeptide deriving from this optimization is Ac-Asp-Glu-Dif-Ile-Cha-Cys-Pro-Cha-Asp-Leu-NH_2, (peptide 9, Table 3, IC_{50} = 1.3 nM). A summary of the optimization process starting from the decapeptide of Landro et al. (*16*) is given in Table 4. Further improvement is possible by introducing in P2−P4

Table 2: Noncoded Amino Acids Used in the Xxx and Ooo Positions

amino acid[a]	code	chirality
γ-carboxyglutamic acid	Gla	L
α-aminobutyric acid	Abu	L
2-aminoisobutyric acid	Aib	L
β-alanine	βAla	L
γ-aminobutyric	γAbu	L
1-amino-1-cyclohexane carboxylic acid	Acx	L
6-aminohexanoic acid	Ahx	L
5-aminovaleric acid	Ava	L
8-aminooctanoic acid	Aoc	L
methionine-DL-sulfoxide	M(O)	L
β-cyclohexyl-alanine	Cha	L+D
norleucine	Nle	L+D
norvaline	Nva	L+D
sarcosine	Sar	L
hydroxyproline	Hyp	L
thioproline	SPro	L
(3*S*,4*S*)-4-amino-3-hydroxy-6-methylheptanoic acid	Sta	
(3*S*,4*S*)-4-amino-3-hydroxy-5-cyclohexylpentanoic acid	Ach	
(3*S*,4*S*)−4-amino-3-hydroxy-5-phenylpentanoic acid	Ahp	
4-carboxymethylpiperazine	Cmpi	L
ornithine	Orn	L
α-diaminopropionic acid	αDP	L
β-diaminopropionic acid	βDP	L
diaminobutyric acid	Dab	L
3-pyridylalanine	Pyr	L+D
homophenylalanine	Hof	L
4-chloro-phenylalanine	Fcl	L+D
4-nitro-phenylalanine	Fno	L
4-fluoro-phenylalanine	Pff	L+D
phenylglycine	Phg	L
1,2,3,4-tetrahydroisoquinoline-3-carboxylic acid	Tic	L+D
3,3-diphenyl-alanine	Dif	L+D
2-naphthylalanine	Nap	L+D
4-thiazolylalanine	Thz	L+D
2-thienyl-alanine	Tha	L
β-cyclopropyl-alanine	Cpa	L
2-aminoindane-2-carboxylic acid	Aic	L
(4-carboxymethyl)-piperidine	Cmp	L
isonipecotic acid	Inp	L
2-aminotetraline-2-acid	Atc	DL
N-(cyclohexyl)-glycine	Chg	
octahydroindole-2-carboxylic acid	Oic	L

[a] Beyond the amino acids listed in the table, all the natural amino acids with the exception of Cys are included in both the L- and the D-configuration. The total number of amino acids used is 91.

the couple D-Glu-Leu (also from our previous work on product inhibitors, ref *11*), yielding Ac-Asp-D-Glu-Leu-Ile-Cha-Cys-Pro-Cha-Asp-Leu-NH_2 (peptide 6 and 7, Table 4, IC_{50} < 200 pM; with our current assays we could not measure the true IC_{50}). Lineweaver−Burk analysis for this inhibitor (peptide 6) was carried out in higher ionic strength conditions (150 mM NaCl), which slightly lower the potency (see below). In these conditions, the measured IC_{50} is 5 nM, and the mechanism is clearly competitive, with K_i = 1.2 nM (Figure 3).

P−P′ Deletions. Deletion of amino acids from the P region of the decapeptides gives a very pattern similar to the one observed for the product inhibitors (*11*), as illustrated in Table 5 (reference peptide 5): deletion of P6 has the maximum effect on activity (peptide 1, 120-fold increase in IC_{50},) and deletion of both P6 and P5 (peptide 2) yield another 20-fold increase. Further shortening has a comparably lower effect, yielding a P3−P4′ heptapeptide (peptide 3) with IC_{50} = 13.5 μM. This is the shortest inhibitor, since neither the P2−P4′ nor the P3−P3′ hexapeptide (peptides 4 and 8) shows activity in our assays. P′-deletions show that P4′ and P3′ give a similar contribution to binding, both yielding a 35-fold decrease in potency (peptides 6 and 7).

Electrostatics of inhibitor binding. (i) Effect of Ionic Strength. As in our previous study of the product inhibitors (*11*), optimization of the P−P′ decapeptide inhibitors was carried out using a low ionic strength buffer: the binding affinity is maximized in these conditions, in line with the electrostatic stabilization observed for the enzyme−substrate complex. We also tested a selection of the peptides resulting from each step of optimization using a higher ionic strength, i.e., in the presence of 150 mM NaCl. The IC_{50}s in both conditions are shown in Table 6. As it might be expected, peptides 2 and 3, which contain a charged residue in P3′, are more sensitive to ionic strength (40-fold ΔIC_{50}) than peptide 1, having Ser in the same position (7-fold ΔIC_{50}). The extent of the ionic strength effect is very similar to the one previously observed for product inhibitors (*11*): the data for the two most potent ones are shown in Table 6 for comparison (peptides 4 and 5). It is apparent that peptide 3 retains low nanomolar potency also in the presence of 150 mM NaCl and represents in both assay conditions the most potent inhibitor of NS3/4A described to date.

(ii) Inhibition of Mutant Enzymes. Modeling of the complex between NS3/4A and the P−P′ inhibitors had suggested that the aspartic acid in position P3′ should interact with Arg109, but could not rule out an alternative interaction with Lys136. Inhibition studies were therefore carried out on NS3/4A mutants in these residues, using high ionic strength conditions to increase the specificity of the electrostatic interactions (see above). While no difference was observed for the lysine mutant (IC_{50} on NS3/4A wt = 5 nM, IC_{50} on NS3/4A[K136M] = 5 nM), a 5-fold difference was found for the arginine mutant (IC_{50} on NS3/4A[R109Q] = 22 nM).

Modeling. We have modeled the interaction of the decapeptide Ac-Asp-Glu-Dif-Ile-Cha-Cys-Pro-Cha-Asp-Leu-NH_2 and NS3/Pep4A by energy minimization and molecular dynamics. The P1′−interaction site is a narrow cleft formed by Lys136 on one side and Gln41 and Thr40 together with a number of polar amino acids on the other side (Figure 4). The lipophilic parts of the side chains of Lys136 and Arg109 create a local environment favorable for hydrophobic residues in P2′. In the case of Cha and phenylglycine, modeling suggests that the cyclic residue is stacked between the side chains of Arg109 and Lys136 so that lipophilic interaction is maximized. By contrast, due to its conformational preferences, this stacking would not be possible for Phe, and we believe this is the reason this amino acid is not preferred at this position (Figure 1). According to the model, backbone hydrogen bonds are formed between the P2′ amino acid and the solvent exposed backbone of Ser41. The presence of the basic amino acids Lys136 and, especially, Arg109 justifies the preference for an acidic amino acid in P3′. Mutagenesis data (see above) disprove an important contribution by Lys136, while confirm a role for Arg109, which is well positioned to form a salt bridge with the P3′ aspartate. In agreement with previous modeling by Landro et al. (*16*), our modeling also suggests that NS4A is involved directly in the formation of the S4′ site. In the area supposed to interact

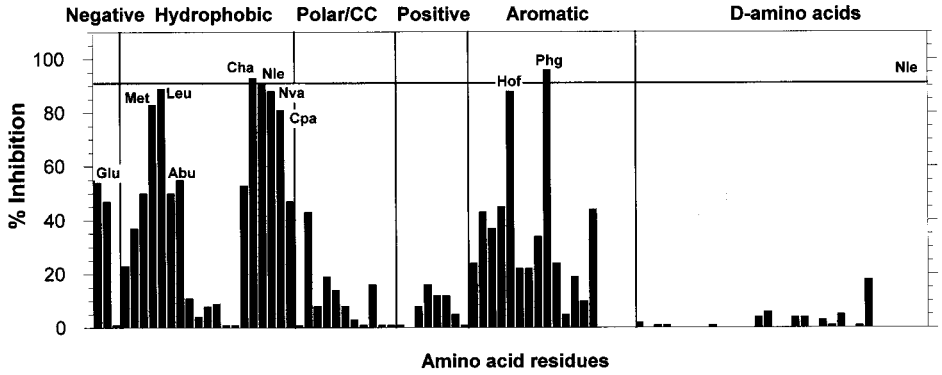

FIGURE 1: Optimization of Position P2′ of the decapeptide inhibitor: screening of the 91 mixtures of the combinatorial library Ac-AspGluDifIleChaCysPro**OooXxx**Leu-NH_2 at the concentration of 1 μM, using the microplate assay (see text). The amino acids included in the Xxx and Ooo positions are shown in Table 2. For easier data readability, amino acids have been grouped according to their physicochemical properties: Negative, Asp, Glu, and Gla; Hydrophobic, Gly (reference), Val, Ile, Met, Leu, Ala, Abu, Aib, βAla, γAbu, Acx, Ahx, Ava, Aoc, M(O), Cha, Nle, Nva, Sar; Polar/Conformationally Constrained, Gln, Asn, Thr, Ser, Pro, Hyp, SPro, Sta, Ach, Acx, Ahp, Cmpi; Positive, Arg, Lys, His, Orn, αDP, βDP, Pyr; Aromatic, Trp, Tyr, Phe, Hof, Fcl, Fno, Pff, Phg, Tic, Dif, Nap, Thz, Tha, Aic, Atc; a few hydrophobic non aromatic residues were added to this group for practical reasons: Cpa, Cmp, Inp, Chg, Oic; D-aa, D-Val, D-Ile, D-Trp, D-Gln, D-Asn, D-Arg, D-His, D-Tyr, D-Pro, D-Phe, D-Met, D-Glu, D-Asp, D-Lys, D-Thr, D-Ser, D-Leu, D-Ala, D-Abu, D-Cha, D-Nle, D-Nva, D-Fcl, D-Phg, D-Tic, D-Dif, D-Pyr, D-Nap, D-Thz, D-Pff. The classes of amino acids are separated by vertical lines, and an horizontal line is drawn at the height of the reference pool corresponding to the parent peptide, in this case P2′ = Nle. For the most active pools, the identity of the amino acid is indicated above the corresponding bar.

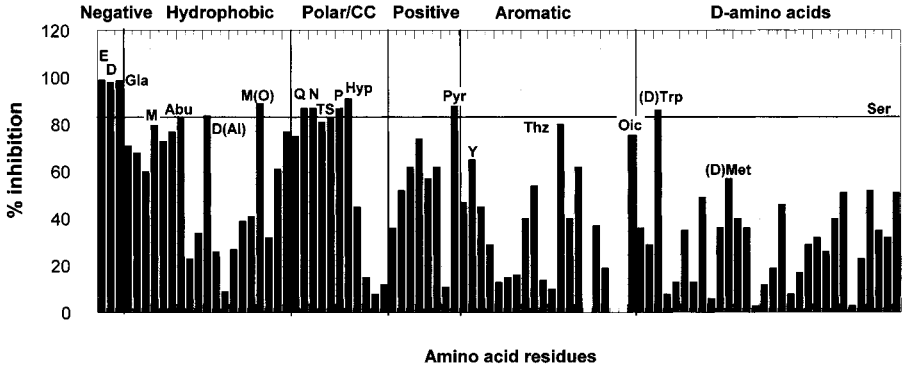

FIGURE 2: Optimization of position P3′ of the decapeptide inhibitor: screening of the 91 analogue set AspGluDifIleChaCysPro[**Cha/Phg/Hof/Nle**]**Ooo**Leu-NH_2. An equimolar mixture of 4 residues, Cha, Phg, Hof, and Nle, was used in position P2′. Each bar in the graph thus represents the cumulative inhibition of the four peptides having either one of the above residues in P2′ and the indicated residue in P3′. All the other conditions are as described in the legend to Figure 1, except the concentration of the peptide pools, which was 0.2 μM. The reference line is drawn at the height of P3′ = Ser.

Table 3: IC_{50} Values for Analogues with Optimized P3′−P4′ Residues

	peptide[a]	IC_{50} (nM)
1.	Ac-AspGluDifIleChaCysProNleSerLeu-NH_2	64
2.	Ac-AspGluDifIleChaCysProNle**Gln**Leu-NH_2	32
3.	Ac-AspGluDifIleChaCysProNle**Hyp**Leu-NH_2	26
4.	Ac-AspGluDifIleChaCysProNle**Asp**Leu-NH_2	1.8
5.	Ac-AspGluDifIleChaCysPro**Cha**SerLeu-NH_2	23
6.	Ac-AspGluDifIleChaCysPro**Cha(D)Trp**Leu-NH_2	820
7.	Ac-AspGluDifIleChaCysPro**ChaGln**Leu-NH_2	14
8.	Ac-AspGluDifIleChaCysPro**ChaHyp**Leu-NH_2	11
9.	Ac-AspGluDifIleChaCysPro**ChaAsp**Leu-NH_2	1.3
10.	Ac-AspGluDifIleChaCysPro**HofGln**Leu-NH_2	18
11.	Ac-AspGluDifIleChaCysPro**HofHyp**Leu-NH_2	15
12.	Ac-AspGluDifIleChaCysPro**HofAsp**Leu-NH_2	1.8
13.	Ac-AspGluDifIleChaCysPro**PhgAsp**Leu-NH_2	7

[a] Abbreviations as in Tables 1 and 2.

Table 4: Summary Table of the Evolution of the Decapeptide Inhibitors

	peptide[a]	IC_{50} (nM)
1.	Ac-GluAspValValAbuCysProNleSerTyr-NH_2	8500
2.	Ac-AspGluDifIleChaCysProNleSerTyr-NH_2	876
2b.	Ac-AspGluDifIleChaCys-NH_2	3100
3.	Ac-AspGluDifIleChaCysProNleSerLeu-NH_2	64
4.	Ac-AspGluDifIleChaCysProChaSerLeu-NH_2	23
5.	Ac-AspGluDifIleChaCysProChaAspLeu-NH_2	1.3
6.	Ac-Asp-D-GluLeuIleChaCysProChaAspLeu-NH_2	<0.2
7.	Ac-Asp-D-GluLeuIleChaCysProChaAspLeuPro-TyrLys(Ac)-NH_2	<0.2

[a] Abbreviations as in Tables 1 and 2.

with P4′, some of the hydrophobic side chains of NS4A are solvent exposed. Moreover, the NS4A binding pocket of the NS3-protease itself is mainly formed by hydrophobic amino acids, some of which (Leu13, Val35, and Leu44) are also solvent exposed and form part of the lipophilic S4′ site. These features would explain the absolute preference for a P4′ hydrophobic amino acids in all natural substrates, confirmed in the present study for the decapeptide inhibitors.

DISCUSSION

In the past few years, remarkable progress has been achieved in elucidating the molecular mechanism by which the NS3/4A protease exerts its activity in the maturation of the HCV polyprotein. Several structures have been reported,

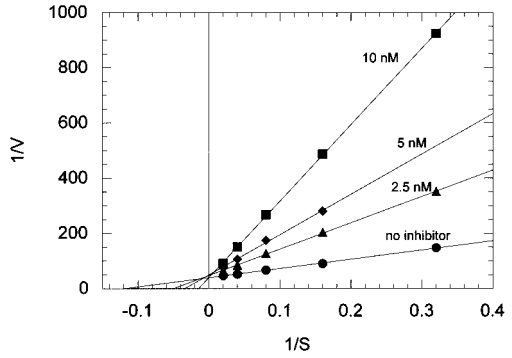

FIGURE 3: Lineweaver-Burk analysis of the optimized P−P′ inhibitor Ac-Asp-D-Glu-Leu-Ile-Cha-Cys-Pro-Cha-Asp-Leu-NH_2 (peptide 6, Table 4) in high ionic strength conditions, showing competitive behavior with $K_i = 1.2$ nM.

Table 5: P and P′ Deletions of Ac-Asp-D-GluLeuGluChaCysProChaAspLeu-NH_2

	peptide[a]	IC_{50} (nM)
1.	Ac-D-GluLeuGluChaCysProChaAspLeu-NH_2	80
2.	Ac-LeuGluChaCysProChaAspLeu-NH_2	1600
3.	Ac-GluChaCysProChaAspLeu-NH_2	13 500
4.	Ac-ChaCysProChaAspLeu-NH_2	na[b]
5.	Ac-Asp-D-GluLeuGluChaCysProChaAspLeu-NH_2	0.63
6.	Ac-Asp-D-GluLeuGluChaCysProChaAsp-NH_2	22
7.	Ac-Asp-D-GluLeuGluChaCysProCha-NH_2	770
8.	Ac-GluChaCysProChaAsp-NH_2	na[b]

[a] Abbreviations as in Table 1. [b] Not active at 100 μM.

Table 6: Comparison of the Potency of the P−P′ Decapeptide Inhibitors in Low and High Ionic Strength Conditions

	peptide[a]	IC_{50} (nM)[b]	IC_{50} (nM)[c] 150 nM NaCl
1.	Ac-Asp-D-GluLeuIleChaCysProNleSer-Leu-NH_2	10	66
2.	Ac-AspGluDifIleChaCysProChaAspLeu-NH_2	1.3	47
3.	Ac-Asp-D-GluLeuIleChaCysProChaAspLeu-NH_2	<0.2	5
4.	Ac-Asp-D-GluLeuIleChaCys-OH	15	120
5.	Ac-Asp-D-GlaLeuIleChaCys-OH	1.5	40

[a] Abbreviations as in Table 1. [b] Experiments were performed using buffer a, see Materials and Methods. [c] Experiments were performed using buffer B, see Materials and Methods.

including the isolated NS3 protease domain with (*19*, *21*) or without (*20*, *22*) a peptide corresponding to the central domain of the NS4A cofactor (Pep4A), the single chain NS3 protease domain/Pep4A (*37*−*39*), and the full-length NS3 protein/Pep4A (*23*). This last paper in particular shows at the molecular level the complex between the protease and the P-region product of the cis cleavage reaction at the NS3/NS4A junction: the C-terminus of NS3 is bound to the active site of the protease domain, in agreement with the previous observation that NS3/4A is inhibited by its own cleavage products (*12*). Product inhibitors derived from the P-region of the substrate have been optimized to low nanomolar potency (*11*, *13*, *14*) and their complex with the NS3 protease domain has been studied in the absence (*18*, *40*, *41*) and presence (*41*) of the Pep4A cofactor. These studies indicate that NS3/4A is an induced fit protease, since binding of both the cofactor and the substrate is required to reduce the conformational flexibility of the enzyme and achieve its cleavage-competent state. In particular, activation of the catalytic machinery of NS3/4A by the P-region of the substrate has been confirmed by the structure of the enzyme covalently bound to reversible inhibitors (*34*, *35*). From the above, it is apparent that the binding mode of the P-region of the substrate and of the corresponding product inhibitors, and the stabilizing effect on the enzyme, are currently known in considerable detail.

By contrast, very little is known about the interaction of the P′-region of the substrate with the S′ region of the enzyme, mainly through indirect enzymological (*15*−*17*) and modeling studies (*16*, *20*, *23*). Interaction with S′ subsites has been shown to contribute significantly to substrate recognition in other serine proteases of the chymotrypsin family (*42*−*44*). For several enzymes of this group, rate acceleration between 2 and 3 orders of magnitude was observed upon optimization of the P1′ or P2′ positions of the substrate, or of P′-side products used in acyl transfer reactions (*43*, *44*). In contrast, the P3′ side chain gave comparatively minor contributions. In the case of NS3/4A protease, the P′-region of the substrate is important for catalysis (as reflected in the contribution to k_{cat}), while most of the energy used for ground-state binding (as reflected in K_m) is extracted by the P-region (*15*−*17*). Accordingly the P′-region of all the natural substrates, in the form of synthetic peptides spanning residues P1′−P10′, does not inhibit NS3/4A (*12*, *18*). As a consequence, P′-region peptides could not be used as a suitable starting point for the development of inhibitors. Therefore, we decided to explore the binding potential of the S′-region of the protease using noncleavable substrate analogues including both P and P′ residues. In the present work we have thus systematically optimized a low-potency ($IC_{50} = 80$ μM), noncleavable decapeptide spanning P6−P4′, derived from the work of Landro et al. (*16*) into a subnanomolar inhibitor, by using single analogues and combinatorial libraries.

The most important criterion in our choice of the P1′ residue was to confer on the scissile bond complete resistance to hydrolysis, even upon prolonged incubation with high concentrations of NS3/4A. As previously noted (*45*), it is possible to mistake simple substrate competition for inhibition, and the rank order of the library pools could then be dependent on assay conditions. In our case, the issue was further complicated by the fact that substrate hydrolysis generates inhibitors in situ (*11*, *12*). We prepared several peptides having *N*-methylated or secondary amino acids in P1′ (Table 1) and set an arbitrary threshold ($k_{cat}/K_m < 100$ M^{-1} s^{-1}) to consider a peptide completely resistant to hydrolysis. This threshold in practice corresponds to the absence of detectable products upon overnight incubation with 10-fold more enzyme than the highest amount used in our assays. Some residues did not meet our criterion, including *N*-methylalanine, when cysteine was the P1 residue and Tic (unlike the findings of ref *16*). The peptides having proline in P1′ were found to be completely stable, and since Pro was also the easiest amino acid from the synthetic point of view, it became our standard in all the subsequent work.

We first examined whether the same pattern of P-region amino acids previously optimized in product inhibitors (*11*) would be effective in these decapeptides as well, and found this to be the case. We then focused our attention to the P4′ residue, based on previous studies (*15*−*17*) showing that it could influence both k_{cat} and K_m of the substrate, and on our observation that Leu was superior to Tyr in this position (*15*). We found here that in the absence of cleavage, P4′ is a key

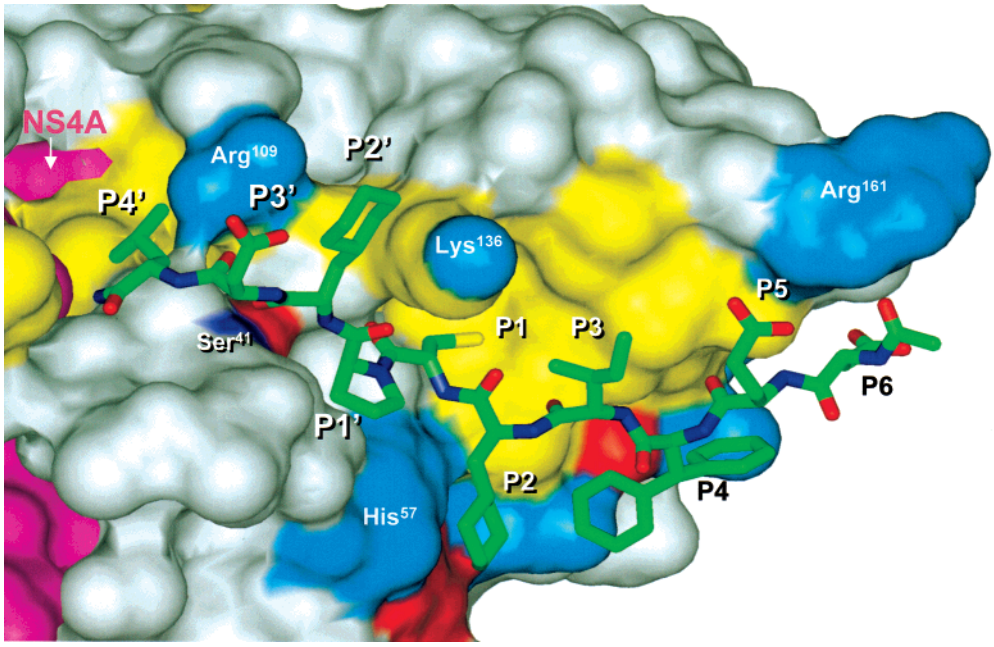

FIGURE 4: Modeling of the P−P′ inhibitor Ac-Asp-Glu-Dif-Ile-Cha-Cys-Pro-Cha-Asp-Leu-NH_2 in the active site of the NS3/4A protease domain, using the coordinates from ref *21*. Color code for NS3/4A: Yellow, hydrophobic, red, negative charge density, blue, positive charge density, magenta, NS4A residues; Color code for the inhibitor: green, carbon, red, oxygen, blue, nitrogen, yellow, sulfur; Hydrogens omitted for clarity.

contributor to binding, yielding a potency increase (10-fold) equivalent to introduction of the whole optimized P4−P2 region. Modeling suggests (ref *16*, this paper) that P4′ is most likely in direct contact with the NS4A cofactor.

Finally, an extensive compilation of the SAR in positions P2′−P3′ was obtained by combinatorial chemistry. Here we found a clear preference for a hydrophobic residue in P2′ and a polar residue in P3′. Similar preferences are found in the presence of turnover, i.e., in the natural substrates of NS3/4A. P2′ is hydrophobic (Met) in NS5A/5B and polar in NS4A/4B (Ser) and NS4B/5A (Gly). All the natural trans cleavage sites have a polar residue in P3′: Ser in NS4B/5A and NS5A/5B, His in NS4A/4B. The NS5A/5B substrate EDVVCCSMSY, featuring in both P2′ and P3′ two of the most preferred residues in our inhibitor library, is the best one in terms of k_{cat} (*46*). Overall, these findings indicate that the binding mode of the inhibitors shares several features with the binding mode of the substrate. This is most apparent in positions P4′ (as discussed above) and P2′, where a modest gain in potency over the best natural residue (Met) was obtained only through the use of noncoded amino acids (Nle, Hof, Phg, and Cha).

At the same time, a new and unexpected preference, which is not observed in any of the natural substrates, was found for an acidic residue (Asp, Glu, or Gla) in position P3′. The change from the best natural residue (Ser) to Asp in P3′ brings about a 30-fold increase in binding (Table 3). In contrast to P2′, our library selected coded amino acids as the most preferred in P3′. It is tempting to speculate that they should necessarily be disfavored by the virus, to allow the P′ substrate region to leave the enzyme after cleavage. This hypothesis is corroborated by the finding that substrate peptides, derived from the sequence of the NS5A/5B junction but incorporating the optimized P2′−P4′ sequence −ChaAsp-Leu−, are turned over with k_{cat} values 10−20-fold lower than the corresponding wild-type substrates (unpublished observations). The preference for an acid does not result from a generic electrostatic effect, akin to the role played by the acidic couple in P6−P5 within the substrate and the product inhibitors (*11*, *12*, *15*−*17*). First, an increase in competing ionic strength does not detract from the potency-enhancing effect of the acid in position P3′: compare peptides 1 and 4, Table 3 with peptides 1 and 3, Table 6. Second, our mutagenesis data and modeling studies strongly suggest that the gain in binding energy results from a specific interaction between the carboxylate and the positive charge of arginine 109. As a consequence, we believe that this interaction may be a novel component of an active-site-directed small molecule inhibitor.

Among the many inhibitors of serine proteases described so far, few make contact with the S′ region of the enzyme (*16*, *45*, *47*−*53*), and most of them do not interact beyond the S1′ subsite (*50*−*52*). Nevertheless, these authors had established that binding to S′ could in principle be exploited for inhibitors. In the case of Proteinase K (*47*, *50*), the inhibitor is actually cleaved while remaining bound to the enzyme (as we observed for one of the NS3/4A inhibitors described by Landro et al.). Imperiali and Abeles (*47*) showed that residues P2′−P3′ in difluoromethyl ketone inhibitors of chymotrypsin, spanning P−P′ could improve potency >1000-fold. The choice of the side chains was based on known inhibitors of the Serpin family. The most direct antecedent of our work was reported by Eichler and Houghten (*45*), who screened a combinatorial hexapeptide library which was biased toward trypsin (preferred P1 residue Arg or Lys) by the presence of lysine as fixed amino acid. Lysine was scanned along the sequence to produce hexapeptides spanning P5−P1 to P1−P5′. The resulting best hexapeptide was P2−P4′, Ac-AKIYRP-NH_2 (IC_{50} = 46 μM). This peptide, however, was still a substrate for the enzyme, being completely hydrolyzed in 4 h (*45*). Moreover, extending the sequence to a dodecapeptide spanning P5−P7′ improved

potency only modestly (Ac-YYGAKIYRPDKM, $IC_{50} = 10$ μM). When combinatorial libraries of peptide inhibitors of chymase and chymotrypsin were prepared (*49*), based on randomization of the P2−P3 or the P1′−P2′ positions, the former yielded 10^3-fold more potent inhibitors (1 nM versus 1 μM K_i for the best compounds).

For NS3/4A, the contribution to binding of the P′-region from a natural HCV cleavage site (NS5A/NS5B) is almost negligible: there is a 3.5-fold difference in potency for the inhibitor spanning P6−P4′ versus the one spanning P6−P1 (compare inhibitor 2 with inhibitors 2b and 5, Table 4). This is because, as already noted (*16*), noncleavable substrate analogues extract most of their binding energy from the P-side. Conversely, the gain in binding energy resulting from our systematic optimization of the P2′−P4′ residues accounts for more than 3 orders of magnitude increase in potency (compare inhibitors 2b and 5, Table 4). The difference in potency between inhibitors containing the natural and the optimal P2′−P4′ moiety is thus >600-fold.

From the perspective of NS3/4A inhibitor design, it is useful to compare the present work with previous studies in this laboratory and elsewhere of the P-region of product inhibitors (*11*−*14*). Optimization of the equivalent region on the P-side (residues P4−P2) had brought about a 20-fold gain in potency (*11*) to be compared with the > 2000-fold gain for P2′−P4′. For the product inhibitors a further 30-fold improvement was obtained by optimizing position P5 (*11*); the P5′ position has not been explored here, although modeling would suggest that additional binding is possible. Moreover, a substantial portion of the binding energy in product inhibitors was extracted by the binding of the C-terminal carboxylate into the active site (*11*, *12*), a feature which is absent from the P−P′ decapeptides. In the absence of the carboxylate contribution, inhibitors binding mainly to the S or S′ subsites of NS3/4A show comparable potency (compare 2b, Table 4, with 2 and 3, Table 5).

Motivation for this study was the hypothesis that a ligand taking advantage of binding to the S′ region of NS3 could interact with the enzyme differently from the substrate, and could represent an entry point for a novel class of NS3 inhibitors. In light of the above, we believe this promise is fulfilled.

ACKNOWLEDGMENT

The authors wish to thank Stefano Acali for help with peptide synthesis, Francesca Naimo and Fabio Bonelli for Mass spectrometry, Silvia Pesci for analytical NMR, Sergio Serafini, Nadia Gennari, Mauro Cerretani, Gabriella Biasiol, and Mirko Brunetti for the protease assays, and Raffaele De Francesco, Victor G. Matassa, and Riccardo Cortese for helpful discussions during the experiments and critical reading of the final manuscript.

REFERENCES

1. Houghton, M. (1996) Hepatitis C Viruses. in *Fields' Virology* (Fields, B. N., Knipe, D. M., and Howley, P. M., Eds.) 3rd ed., pp 1035−1058, Lippincott-Raven, Philadelphia, New York.
2. Hoofnagle, J. H. (1997) *Hepatol. 26* (Suppl. 1), 15S−20S.
3. Bartenschlager, R., Ahlborn Laake, L., Mous, J., and Jacobsen, H. (1994) *J. Virol. 68*, 5045−5055.
4. Lin, C., Pragai, B. M., Grakoui, A., Xu, J., and Rice, C. M. (1994) *J. Virol. 68*, 8147−8157.
5. Tanji, Y., Hijikata, M., Hirowatari, Y., and Shimotohno, K. (1994) *Gene 145*, 215−219.
6. Failla, C., Tomei, L., and De Francesco, R. (1995) *J. Virol. 69*, 1769−1777.
7. Hahm, B., Han, D. S., Back, S. H., Song, O. K., Cho, M. J., Kim, C. J., Shimotohno, K., and Jang, S. K. (1995) *J. Virol. 69*, 2534−2539.
8. Han, D. S., Hahm, B., Rho, H. M., and Jang, S. K. (1995) *J. Gen. Virol. 76*, 985−993.
9. Nedderman, P., Tomei, L., Steinkühler, C., Gallinari, P., Tramontano, A., and De Francesco, R. (1997) *J. Biol. Chem. 378*, 469−476.
10. Failla, C., Tomei, L., and De Francesco, R. (1994) *J. Virol. 68*, 3753−3760.
11. Ingallinella, P., Altamura, S., Bianchi, E., Taliani, M., Ingenito, R., Cortese, R., De Francesco, R., Steinkühler, C., and Pessi, A. (1998) *Biochemistry 37*, 8906−8914.
12. Steinkühler, C., Biasiol, G., Brunetti, M., Urbani, A., Koch, U., Cortese, R., Pessi, A., and De Francesco R. (1998) *Biochemistry 37*, 8899−8905.
13. Llinas-Brunet, M., Bailey, M., Fazal, G., Goulet, S., Halmos, T., Laplante, S., Maurice, R., Poirier, M., Poupart, M. A., Thibeault, D., Wernic, D., and Lamarre, D. (1998) *Bioorg. Med. Chem. Lett. 8*, 1713−1718.
14. Llinas-Brunet, M., Bailey, M., Déziel, R., Fazal, G., Gorys, V., Goulet, S., Halmos, T., Maurice, R., Poirier, M., Poupart, M. A., Rancourt, J., Thibeault, D., Wernic, D., and Lamarre, D. (1998) *Bioorg. Med. Chem. Lett. 8*, 2719−2724.
15. Urbani, A., Bianchi, E., Narjes, F., Tramontano, A., De Francesco, R., Steinkühler, C., and Pessi, A. (1997) *J. Biol. Chem. 272*, 9204−9209.
16. Landro, J. A, Raybuck, S. A, Luong, Y. P. C., O'Malley, E. T., Harbeson, S. L., Morgenstern, K. A., Rao, G., and Livingston, D. J. (1997) *Biochemistry 36*, 9340−9348.
17. Zhang, R., Durkin, J., Windsor, W. T., McNemar, C., Ramanathan, L., and Le, H. V. (1997) *J. Virol. 71*, 6208−6213.
18. La Plante, S. R., Cameron, D. R., Aubry, N., Lefebvre, S., Kukolj, G., Maurice, R., Thibeault, D., Lamarre, D., and Llinàs-Brunet, M. (1999) *J. Biol. Chem. 274*, 18618−18624.
19. Kim, J. L., Morgenstern, K. A., Lin, C., Fox, T., Dwyer, M. D., Landro, J. A., Chambers, S. P., Markland, W., Lepre, C. A., O'Malley, E. T., Harbeson, S. L., Rice, C. M., Murcko, M. A., Caron, P. R., and Thomson, J. A. (1996) *Cell 87*, 343−355.
20. Love, R. A., Parge, H. E., Wickersham, J. A., Hostomska, Z., Habuka, N., Moomaw, E. W., Adachi, T., and Hostomska, Z. (1996) *Cell 87*, 331−342.
21. Yan, Y., Li, Y., Munshi, S., Sardana, V., Cole, J., Sardana, M., Steinkühler, C., Tomei, L., De Francesco, R., Kuo, L., and Chen, Z. (1998). *Protein Sci. 7*, 837−847.
22. Barbato, G., Cicero, D. O., Nardi, M. C., Steinkühler, C., Cortese, R., De Francesco, R., and Bazzo, R. (1999*) J. Mol. Biol. 289*, 370−384.
23. Yao, N., Reichert, P., Taremi, S. S., Prosise, W. W., and Weber, P. (1999) *Structure 7*, 1353−1363.
24. Atherton, E., and Sheppard, R. C. (1989) *Solid-phase peptide synthesis, a practical approach*, IRL Press, Oxford.
25. Wallace, A., Altamura, S., Toniatti, C., Vitelli, A., Bianchi, E., Delmastro, P., Ciliberto, G., and Pessi, A. (1994) *J. Pept. Res. 7*, 27−31.
26. Bianchi, E., Folgori, A., Wallace, A., Nicotra, M., Acali, S., Phalipon, A., Barbato, G., Bazzo, R., Cortese, R., Felici, F., and Pessi, A. (1995) *J. Mol. Biol. 247*, 154−160.
27. Wallace, A., Koblan, K. S., Hamilton, K., Marquis-Omer, D. J., Miller, P., Mosser, S. D., Omer, C. A., Schaber, M. D., Cortese, R., Oliff, A., Gibbs, J. B., and Pessi, A. (1996) *J. Biol. Chem. 271*, 31306−31311.
28. Becker, J. A., Wallace, A., Garzon, A., Ingallinella, P., Bianchi, E., Cortese, R., Simonin, F., Kieffer, B., and Pessi, A. (1999) *J. Biol. Chem. 274*, 27513−27522.

29. Sole, N. A. and Barany, G. (1992) *J. Org. Chem. 57*, 5399−5403.
30. De Francesco, R., Urbani, A., Nardi, M. C., Tomei, L., Steinkühler, C., and Tramontano, A. (1996) *Biochemistry 35*, 13282−13287.
31. Bianchi, E., Urbani, A., Biasol, G., Brunetti, M., Pessi, A., De Francesco, R., and Steinkühler, C. (1997) *Biochemistry* 36, 7890−7897.
32. Cerretani, M., Di Renzo, L., Serafini, S., Vitelli, L., Gennari, N., Bianchi, E., Pessi, A., Urbani, A., Colloca, S., De Francesco, R., Steinkühler, C., and Altamura, S. (1999) *Anal. Biochem. 266*, 192−197.
33. Halgren, T. A. (1996) *J. Comput. Chem. 17*, 490−519.
34. Barbato, G., Cicero, D. O., Cordier, F., Narjes, F., Gerlach, B., Sambucini, S., Grzesiek, S., Matassa, V. G., De Francesco, R., and Bazzo, R. (2000) *EMBO J. 19*, 1195−1206.
35. Di Marco, S., Rizzi, M., Volpari, C., Walsh, M. A., Narjes, F., Colarusso, S., De Francesco, R., Matassa, V. G., and Sollazzo, M. (2000) *J. Biol. Chem. 275*, 7152−7157.
36. Houghten, R. A., Pinilla, C., Blondelle, S. E., Appel, J. R., Dooley, C. T., and Cuervo, J. H. (1991) *Nature 354*, 84−86.
37. Pasquo, A., Nardi, M. C., Dimasi, N., Tomei, L., Steinkühler, C., Delmastro, P., Tramontano, A., and De Francesco, R. (1998) *Folding Des. 3*, 433−441.
38. Taremi, S. S., Beyer, B., Maher, M., Yao, N., Prosise, W., Weber, P. C., and Malcom, B. A. (1998) *Protein Sci. 7*, 2143−2149.
39. Howe, A. Y., Chase, R., Taremi, S. S., Risano, C., Beyer, B., Malcolm, B., and Lau, J. (1999) *Protein Sci. 8*, 1332−1341.
40. Cicero, D. O., Barbato, G., Koch, U., Ingallinella, P., Bianchi, E., Nardi, M. C., Steinkühler, C., Cortese, R., Matassa, V. G., De Francesco, R., Pessi, A., and Bazzo, R. (1999) *J. Mol. Biol. 289*, 385−396.
41. Bianchi, E., Orru′, S., Dal Piaz, F., Ingenito, R., Casbarra, A., Biasiol, G., Koch, U., Pucci, P., and Pessi, A. (1999) *Biochemistry 38*, 13844−13852.
42. Chagas, J. R., Hirata, I. Y., Juliano, M. A., Xiong, W., Wang, C., Chao, J., Juliano, L., and Prado, E. S. (1992) *Biochemistry 31*, 4969−4974.
43. Schellenberger, V. Turk, C., and Rutter, W. J. (1994) *Biochemistry 33*, 4251−4257.
44. Le Bonniec, B. F., Myles, T., Johnson, T., Knight, C. G., Tapparelli, C., and Stone, S. (1996) *Biochemistry 35*, 7114−7122.
45. Eichler, J., and Houghten, R. A. (1993) *Biochemistry 32*, 11035−11041.
46. Steinkühler, C., Urbani, A., Tomei, L., Biasiol, G., Sardana, M., Bianchi, E., Pessi, A., and De Francesco, R. (1996) *J. Virol. 70*, 6694−6700.
47. Imperiali, B., and Abeles, R. H. (1987) *Biochemistry 26*, 4474−4477.
48. Betzel, C., Singh, T. P., Visanji, M., Peters, K., Fittkau, S., Saenger, W., and Wilson, K. S. (1993) *J. Biol. Chem. 268*, 15854−15858.
49. Bastos, M., Maeji, N. J., and Abeles,, R. H. (1995) *Proc. Natl. Acad. Sci U.S.A. 92*, 6738−6742.
50. Saxena, A. K., Singh, T. P., Peters, K., Fittkau, S., and Betzel, C. (1996) *Protein Sci. 5*, 2453−2458.
51. Tong, L., Qian, C., Massariol, M.-J., Déziel, R., Yoakim, C., and Lagacé, L. (1998) *Nat. Struct. Biol. 5*, 819−826.
52. Abato, P., Conroy, J. L., and Seto, C. T. (1999) *J. Med. Chem. 42*, 4001−1009.
53. Speri, S., Jacob, U., de Prada, N. U., Stürzenbecher, J., Wilhelm, O. G., Bode, W., Magdolen, V., Huber, R., and Moroder, L. (2000) *Proc. Natl. Acad. Sci. U.S.A. 97*, 5113−5118.

BI001590G